Ultrasensitive and Selective Bacteria Sensors Based on Functionalized Graphene Transistors

Xuebin Tan, Minye Yang, Liang Zhu, Gayathri Gunathilake, Zhixian Zhou, Pai-Yen Chen, Yifan Zhang, and Mark Ming-Cheng Cheng

***Abstract*—We propose here a graphene biosensor based on the field-effect transistor (FET) architecture for continuous and real-time monitoring of bacteria, with beneficial features including facile operation, low-cost, selectivity, and high sensitivity. Our sensing device consists of the chemical-vapor-deposition (CVD) graphene monolayer, functionalized by the phage tail spike proteins (TSPs) that form specific binding sites to capture E. coli bacteria. We have investigated effects of surface functionalization and bacteria binding on the conductance of atomically thin graphene that determines transfer characteristics of a graphene FET (GFET). We have experimentally demonstrated that the concentration of E. coli bacteria can be selectively and accurately detected (at the single bacterium level) by a TSP-functionalized GFET. The proposed graphene biosensor may be of great interest for rapid, efficient detection of bacterial pathogens that could potentially pose a severe threat to human, animal, or plant health.**

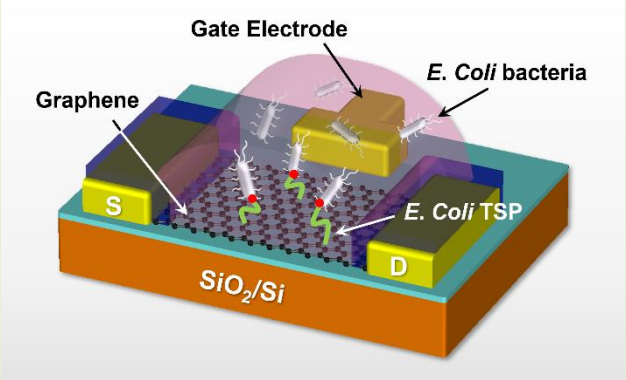

***Index Terms*—Graphene field-effect transistors, biosensors, bacteria monitoring, E coli bacteria,**

I. Introduction

HUMAN pathogenic bacteria, such as E. coli, Salmonella, Listeria, and Staphylococcus, are often excreted by warm-blooded animals and survive well in the warm and moisture environment. They can contaminate urban surface water through human and animal fecal waste and stormwater runoff, which lead to serious consequences. The traditional microbiological methods, such as polymerase chain reaction (PCR), enzyme-linked immunosorbent assay (ELISA), and deoxyribonucleic acid (DNA) hybridization, either are labor-intensive or require bulky and expensive instruments [1], [2]. Recently, biosensors based on solid-state electronic devices have attracted wide interests, since they may offer great advantages over the traditional methods, such as the ease of operation, short turnaround time, and wide detection capacity. Graphene has emerged as a promising carbon material for biosensors, due to its two-dimensional atomic structures that enable large reactive surfaces and efficient chemical doping, as well as the potential for increased sensitivity to electrochemical reactions. Graphene has a gapless band structure and a finite density of states around the Dirac point, which leads to a widely tunable electrical conductivity, sensitively responsible for chemical and electrostatic gating effects. Graphene-based micro-/nano-sensors have been developed to detect gases and biomolecular agents, with a molecular level sensitivity and multifunctionality [3]–[19]. Very recently, we have shown that combining unique electronic and chemical features of a GFET can be exploited to build a chemically-tuned radio-frequency (RF) modulator [20], in which an input RF signal can be efficiently converted to the second harmonic, with a conversion gain controlled by the chemical doping effect. Such an RF biosensor, only possible with GFETs, shows great potential to be implemented as ultrasensitive, low-cost, and low-profile wireless biochemical and gas sensors, as well as smart wearables [21]–[23].

Berry's group first reported the use of graphene-based biosensors for single bacteria detection [24]. However, their approach was based on the electrostatic adhesion of bacteria on a pristine graphene, which is non-specific (i.e., charged bacteria of different types cannot be separately perceived), thus not applicable to practical sensing applications. Recent

Xuebin Tan is with the Intel Corporation, Santa Clara, CA, 95054, USA. (e-mail: xuebin.tan@intel.com)

Minye Yang, Liang Zhu and Pai-Yen Chen are with the Department of Electrical and Computer Engineering, University of Illinois at Chicago, Chicago, IL 60607, USA. (e-mail: myang66@uic.edu; pychen@uic.edu).

Gayathri Gunathilake is with the Department of Food Science and Human Nutrition, Michigan State University, East Lansing, MI, 48824, USA. (e-mail: gunathil@msu.edu)

Zhixian Zhou is with the Department of Physics, Wayne State University, Detroit, MI, 48202, USA. (e-mail: zxzhou@wayne.edu)

Yifan Zhang is with the Department of Food and Nutrition, Wayne State University, Detroit, MI, 48202, USA (e-mail: yifan.zhang@wayne.edu)

Ming-Cheng Cheng is with the Department of Electrical and Computer Engineering, University of Alabama, Tuscaloosa, AL, USA. (e-mail: mmcheng@ua.edu)

breakthrough shows that in interaction between biomaterials and graphene can be utilized as a nanosensor platform for monitoring the bacteria growth on tooth enamel [25]. In this proof-of-concept demonstration, bio-selective detection of bacteria at single-cell levels was achieved by using the self-assembly antimicrobial peptides on graphene. Similarly, it has been recently demonstrated that graphene-based biosensors can detect E. coli bacteria [26], with a high sensitivity and a limit of detection (LOD) of 10 cfu/mL.

Conventionally, the immobilization of P22 tail spike proteins (TSPs) [27] functionalized on the silicon substrate has been used for selective bacterial sensing [28]. However, to date, surface functionalization of graphene monolayer with TSPs has not been studied yet. In this work, we will investigate, for the first time, sensing mechanism and selectivity of the TSP-functionalized GFET used for the detection of E. coli bacteria. The goal of this study is to demonstrate that a TSP-functionalized GFET can provide highly selective detection of E. coli bacteria, for which the engineered TSPs form binding sites to enable identification and characterization of molecular determinants of bacterial host specificity. Each TSP as a receptor has two terminal domains, where the C-terminal domain can bind to the cellular Lipopolysaccharides (LPS) receptor, while the N-terminal domain can be immobilized to the biosensor substrate through 1-Ethyl-3-(3-dimethylaminopropyl)-carbodiimide/N-hydroxy-succinimide (EDC/NHS) [27]. Attaching TSPs to the flatland sensor, ion-sensitive GFET [Fig. 1] may allow an increased area for electronic interactions between the bacteria and the graphene channel. Moreover, the anchoring of TSPs to the substrates allows correct orientation of TSPs. Hence, the C-terminal binding domains of TSPs are exposed to the bacterial surface, which may increase the binding efficiency of ligand-receptor and the smoothness of surface for facilitating characterization.

II. Results and Discussions

Figure 1(a) shows the macroscopic image of a GFET-based bacteria sensor. Figure 1(b) schematically shows the experimental setup, where the channel conductance of GFETs is determined by the number of bacteria trapped on the functionalized graphene surface; the optical images and its zoom-in view of the fabricated GFET are shown in Figs. 1(c) and 1(d). The Raman spectrum measurement, shown in Fig. 1(e), reveals that most areas (80-85%) of GFET's channel are single layer graphene. Binding of the bacteria was monitored by measuring variations in the electrical conductance of graphene, i.e., drain-current (I_{DS}) versus gate-voltage (V_{GS}) curves. Figure 1(b) also shows the measurement setup, where the bacteria sensing was conducted in the liquid environment. When the device is immersed in a liquid solution, charges on the cellular membranes of bacteria will affect local dipoles and thus surface potential of graphene [29]. Similar to the pH sensing mechanism, when the negatively charged bacteria are attached to the graphene surface, the Dirac point of graphene, corresponding to the dip of drain current, is expected to shift to higher positive gate voltages, owing to the increased amount of hole (p-type doping) in the graphene channel. On the other hand, if the bacteria are positively charged, the Dirac point will shift to the left because, in this scenario, electrons (n-type

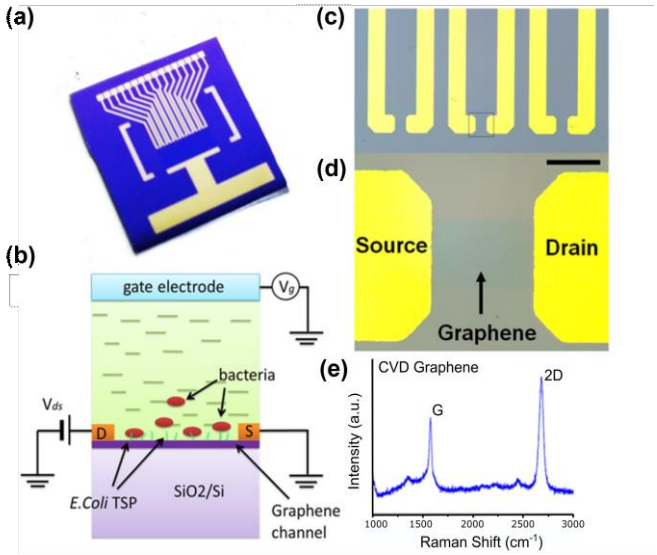

Fig. 1. Graphene bacteria sensor and electrical measurement setup. (a) Optical image of an GFET as a compact bacteria sensor; (b) measurement setup for GFET biosensor; (c), (d) zoom-in microscope images of the device (scale bar represents 40 μm); (e) Raman spectrum of the chemical vapor deposition (CVD) graphene.

doping) are induced in the graphene channel. In this case, since the functionalized TSPs will form the binding sites for the molecular determinants inside the bacterial host that is larger than the Debye length [30], the Debye screening effect may hardly prevent the charged determinants doped in graphene. In our experiment, an Ag/AgCl reference electrode was used to avoid the potential change due to electrochemical reactions. By sweeping the top gate voltage and monitoring the drain current, one should be able to measure the shift of Dirac point of GFET exposed to different bacterial samples.

Figure 2 shows the flow chart for the surface functionalization of graphene and schematics of how the E. coli bacteria is captured by the E. coli TSPs functionalized on the graphene surface. First, we treated the graphene with oxygen plasma for 2 seconds, for introducing more oxygen and hydroxyl groups at its defect sites [Fig. 2(a)]. Then, the graphene was immersed in a 2% solution of (3-Aminopropyl)triethoxysilane (APTES) in ethanol (95%) with a pH value of 5 for 15 minutes. The device was baked at 100°C for 5 minutes for curing the silane monolayer and was rinsed again with ethanol and deionized (DI) water. To activate the amine group of the APTES [Fig. 2(b)], the graphene device was incubated in 2% glutaraldehyde for 30minutes at room temperature. During this step, the amine group will form C=N group with the carboxyl group of the glutaraldehyde [Fig. 2(c)]. Also, the other terminal of the glutaraldehyde can be used for the bioconjugation with a TSP through its N-terminal [Fig. 2(c)]. The 180 μg/ml ~ 400 μg/ml E. coli TSPs were used to functionalize the graphene through bioconjugation [Fig. 2(d)]. After the TSPs immobilization, 1% bovine serum albumin (BSA) was used to block the nonspecific binding [Fig. 2(e)]. Details for the preparation of GFET and TSP can be found in the Appendix A. To prepare the E. coli O157 bacteria, a single colony of E. coli O157 ATCC70926 was inoculated in 10 ml of Luria-Bertani (LB) broth and incubated overnight at 37°C.

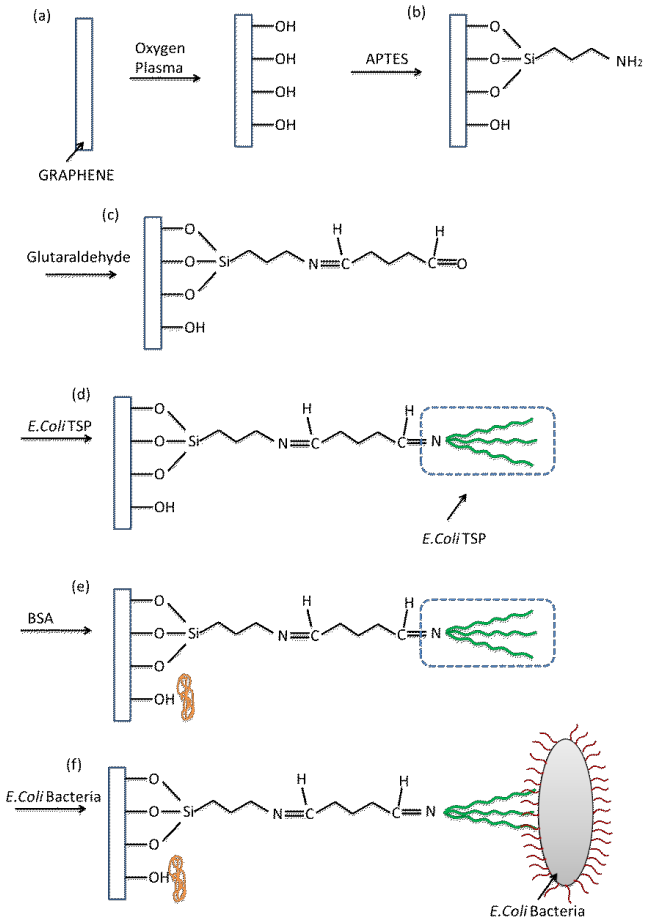

Fig. 2. Flow chart of surface functionalization of graphene: (a) oxygen plasma treatment for introducing the surface oxygen and hydroxyl group; (b) APTES reaction for introducing the amine group; (c) binding of glutaraldehyde that introduces the carboxyl group; (d) E. coli TSPs immobilization with the carboxyl groups; (e) 1% BSA was applied for blocking unconjugated sites; (f) schematics of E. coli bacteria binds to E. coli TSP.

Bacterial suspension was centrifuged at 5000 rpm for 5 minutes and washed twice with 0.85% saline. To measure the binding of the bacteria with the graphene biosensor, a droplet of fresh E. coli bacteria with a concentration of 1×10^{9}~1×10^{10} cfu/ml was deposited to cover the functionalized graphene. After 30 minutes, we washed off the non-binding bacteria by rinsing the device with tap water. The electrical conductance of the device in response to the bacteria binding was measured by and Ag/AgCl reference gate electrode, as shown in Fig. 1(b). The semiconductor characterization system (Keithley 4200) was used to measure I_{DS}~V_{GS} characteristics of the GFET-based biosensor in a liquid (tap water) environment.

The electrochemical properties of the E. coli bacteria were characterized using the zeta potential, which is the electrical potential between the aqueous solution and the stationary layer of the surrounding liquid attached to the bacteria [21]-[23]. The zeta potential measurement was based on the phase analysis light scattering (PALS) in Zetasizer Nano ZEN3600. The E. coli bacteria and E. coli TSP were diluted with tap water and the zeta potential was measured in Malvern capillary plastic cells (DTS 1061). The scattering detection angle is 173 and the

TABLE I
ZETA POTENTIAL OF E. COLI BACTERIA, E. COLI PHAGE, BSA, AND E. COLI TSP IN THE TAP WATER

Sample Name	Zeta Potential (mV)	Mobility (cm^2/Vs)	Conductivity (mS/cm)
E. coli bacteria	0.328 ~ 0.517	0.0257 ~ 0.0406	1.67 ~ 0.401
BSA	−13.1 ~ −15.8	−1.03 ~ −1.24	0.324 ~ 1.02
E. coli phage	−12.2 ~ −17.3	−0.954 ~ −1.354	0.396 ~ 1.69
E. coli TSP	−2.88 ~ −15.8	−0.226 ~ −1.236	0.158 ~ 6.71

zeta potential value was calculated from the Smoluchowski equation using Malvern software. Zeta potential of each material (TSP, BSA, and bacteria) were measure in the tap water at 25°C, and results are summarized in Table 1. We have diluted original samples into 10 times and 100 times with the tap water. It was found that the E. coli bacteria have a zeta potential around 0.328 mV to 0.517 mV in the tap water [Table 1], implying that the surface charge of the bacteria in the tap water environment is positive. We notice that some literature shows that zeta potential of the bacteria is negative [24]-[26]. This is because the zeta potential depends on the pH or the ion concentration of the background media.

We have systematically studied the carrier transport properties in the functionalized GFET before and after exposure to the E. coli bacteria. We used 1% BSA to quench the unreacted E. coli TSPs immobilized on the surface of graphene. In addition, we have conducted a series of comprehensive experiments for testing the selectivity of bacterial binding; here two different types of bacteria, Salmonella and E. coli, were measured using the same TSP-functionalized GFET. The E. coli TSPs may efficiently capture the E. coli bacteria as expected, while being inactive to the Salmonella bacteria. Figure 3(a) presents transfer characteristics of the GFET biosensors during the surface functionalization and tentative binding of Salmonella bacteria; here the I_{DS}~V_{GS} curve of TSP-functionalized GFET was measured as the baseline. It is seen from Fig. 3(a) that the BSA blocking did not shift the Dirac point (current dip in the I_{DS}~V_{GS} curve), indicating that the BSA blocking has no effect on the TSP-immobilized graphene surface and, therefore, the conductance of graphene remains unchanged. When 5×10^{10} cfu/mL Salmonella bacteria were added onto the graphene channel, it caused no significant shift of the Dirac point, as can be seen in Fig. 3(a). This is because the Salmonella bacteria are not able to bind to the E. coli TSPs, due to their mismatched biofunctional groups. Also, the non-specific binding of the Salmonella bacteria was prevented by the BSA blocking. Figure 3(b) presents the microscope image of the GFET biosensor after exposure to the Salmonella bacteria, showing that Salmonella bacteria were not bound to the E. Coli TSPs. Figure 3(c) presents the transfer curve for a TSP-functionalized GFET bound with the E. coli bacteria; here we cultured the E. coli bacteria onto the graphene channel and used the saline solution to remove the unbounded E. coli bacteria. It is clearly seen from Fig. 3(c) that, in sharp contrast to the exposure of Salmonella bacteria, binding of E. coli bacteria can cause the n-type chemical doping effect, leading to a negative shift of the Dirac point (-20 mV). This can be attributed to the fact that the positively charged bacteria would

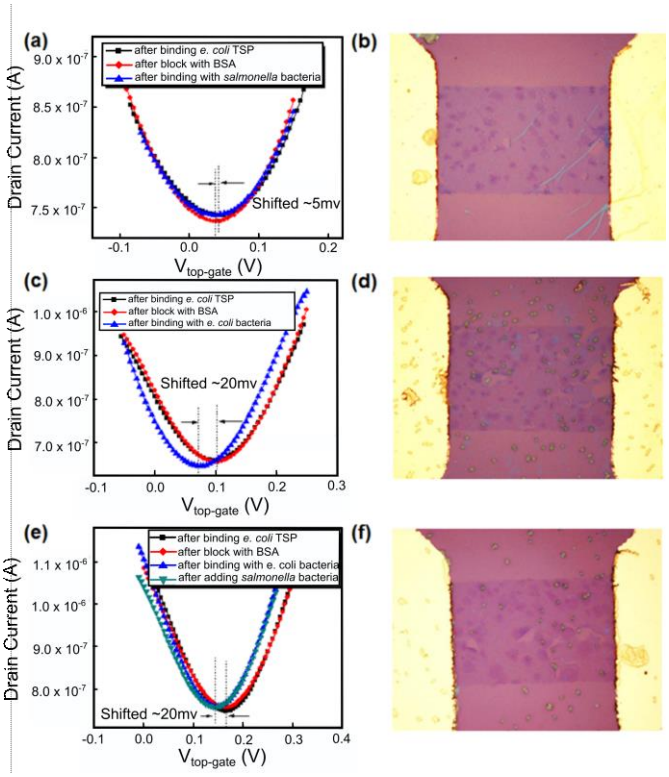

Fig. 3. (a) I_{DS} ~ V_{GS} characteristics of a GFET before and after exposure to the Salmonella bacteria, showing that no Salmonella bacteria can be trapped by the TSP sites of graphene. (b) Optical microscope image of the GFET after exposure to the Salmonella bacteria. (c) I_{DS} ~ V_{GS} characteristics before and after the binding of E. coli bacteria, showing that Dirac point of GFET was shifted by ~20mV. (d) Optical microscope image of the GFET in (c) after binding of the E. coli bacteria; there are about 33±2 bacteria counts. (e) I_{DS} ~ V_{GS} characteristics for the same device in (c), after successive exposures to the E. coli bacteria and the Salmonella bacteria, showing that the Salmonella bacteria has no effect on conductance of the graphene channel. (f) Optical microscope image of the GFET in (e), after adding the Salmonella bacteria; there are about 27±2 E. coli bacteria counts tightly bound to E. coli TSPs on the graphene surface.

induce electrons (n-type doping) in the graphene channel, according to the measurement of the E. coli bacteria [Table 1]. We also calculated the electron and hole mobilities in the GFET, which can be derived as $\mu = (1/C_g)(\delta\sigma/V_g)$ [37], where C_g is the quantum capacitance of the graphene (~20 nFcm^{-2}), σ is the conductance, and V_g is the gate voltage [38], [39]. The calculated hole and electron mobilities are nearly the same (1.1×10^3 ~ 1.2×10^3 cm^{2}V^{-1}s^{-1}), due to the linear, symmetric energy dispersion of graphene. Figure 3(d) is the microscope image of a GFET biosensor exposed to the E. coli bacteria. Based on the microscope image, the number of the E. coli bacteria trapped on to the 80 μm × 50 μm graphene channel was counted as 33 ± 2. Finally, we rinsed the GFET biosensor in Fig. 3(c) with the saline solution and cultured the Salmonella bacteria on it. Figures 3(e) and 3(f) present the transfer curve and the microscope image after further exposure to the Salmonella bacteria. We found that there is hardly to observe any shift in the Dirac point after adding the Salmonella bacteria onto the GFET biosensor that is already E. coli-bound. As a result, it is evident that the biospecific binding and thus

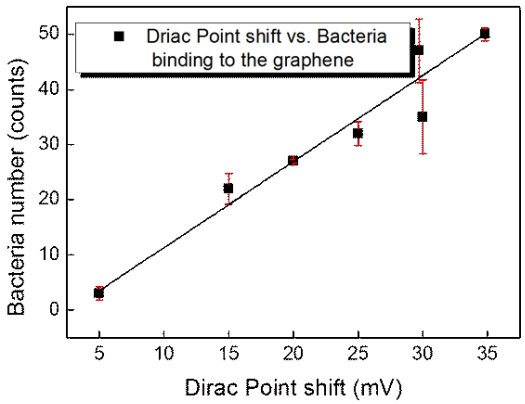

Fig. 4. Dirac point shift as a function of the number of bacteria bound to the GFET; here seven different biosensors were measured to obtain the statistic information. The sensitivity extracted from the linear fitting is 1.24 mV/E. coli bacteria.

selective detection of bacteria is possible with the GFET biosensor, where the conductive channel is made of a single layer of carbon atoms, which can be readily functionalized by specific biomarker, such as TSPs used here.

Figure 4 summarized the sensitivity of this GFET-based bacteria sensor as a function of the number of the E. coli bacteria captured by the E. coli TSPs, showing an excellent linearity and a sensitivity 1.24 mV/bacteria. With a high population (~50) of bacteria bound to the graphene surface, the Dirac point shift can be up to 35 mV. The results in Fig. 4 validate that the TSP-functionalized GFET could offer selective detection for the GFET-based sensor, showing the potential for detection of bacterial pathogens with certain selectivity.

At last, it should be noted that this TSP-functionalized GFET may also be able to mitigate the electrolytic noise and drift issue at the graphene interface, thanks to the selectivity of the TSP-functionalized GFET sensor and the blocking of the non-specific binding on graphene surface enabled by BSA. Additionally, we note that the sensitivity of accuracy of detecting analytes can be improved by increasing the number of TSPs functionalized on the graphene surface, or by designing top-gate and/or double-gate GFET with suitable electrode materials.

III. Conclusions

In this paper, we have demonstrated a label-free, graphene transistor-based bacteria sensor, which can detect specific enteric bacteria, such as E. coli and Salmonella bacteria, depending on the surface functionalization method used to sensitize graphene. Specifically, we have developed an efficient method to develop TSPs-functionalized GFET that enables highly selective binding of the E. coli bacteria. We have measured variations in transfer characteristics (I_{DS}~V_{GS} curves) of a GFET for all functionalization steps and molecular binding

events and have retrieved the sensitivity by analyzing the shift of Dirac point in response to the number of the bacteria bound onto the graphene surface. Our results show that a sensitivity of 1.24 mV/bacteria and a good linearity can be achieved, with excellent selectivity to the E. coli bacteria. The proposed GFET-based biosensor shows great potential as a molecular diagnostic system to identify dangerous bacteria, such as E. coli, staph infections, human/animal pathogen, and even some superbugs. Further development may lead to contactless RF biosensors, taking advantages of GFET's biosensing and ambipolar frequency doubling functions, for meeting unprecedented rise in the demand for wireless wearables and implants, healthcare internet-of-things, and radio-frequency identification (RFID) sensors.

APPENDIX

A. Device Fabrication

We used chemical vapor deposition (CVD) method to grow pristine graphene [40]. Typically, a 25 μm thick copper foil (Alfa Aesar) was loaded into a furnace. The system was pumped down in vacuum (10^{-4} Torr) and copper was annealed at 1000°C with 3 standard cubic centimeters per minute (sccm) hydrogen gas first. The graphene was synthesized by adding the mixture of methane and hydrogen gases with a ratio of flow rates 10:1 (CH_4:H_2). When the temperature was above 700°C, methane was thermally decomposed into carbon and hydrogen on top of copper surfaces. Due to the limited solubility of carbon atoms in copper, a single-layer graphene was formed. Figure 5 shows the fabrication process flow chart of GFET, which is similar to that of our recently developed pH sensors [7]. The CVD graphene was first transferred onto a silicon substrate with 300 nm silicon dioxide (SiO_2). Then 200 nm thick polymethylmethacrylate (PMMA) was spin-coated on top of the graphene/copper. Afterward, the backside graphene was etched using the oxygen plasma (100W O_2 30 sccm 30 s), and the copper foil was etched by a diluted copper etchant (APS-100). To remove the metal residual and other polymer contamination on the graphene, a modified RCA clean was used to clean the graphene before being transferred to the substrate [41]. After rinsing with DI water, the PMMA/graphene sheet was carefully taken out of the DI water and gently attached to the target substrate. The PMMA was dissolved using the acetone solution right after the PMMA/graphene sheet was air dried. The patterning of graphene was done by the photolithography and the oxygen plasma etching, in order to define the graphene channel (rectangular shape with length of 80 μm and width of 50 μm). Finally, a thin layer of Ti/Au (5 nm/50 nm) was deposited as the drain and source electrodes using the e-beam evaporation and the lift-off process. In our design, both back gate (silicon) and top gate (reference electrode) could be applied voltage to tune conductivity in graphene.

B. Preparation of phage ΦV10

Phage ΦV10 is an E. coli O157-specific phage and encodes a tail spike that specifically recognizes the O157 antigen of E. coli O 157 [42], [43]. 100 μl of E. coli O157 ATCC700926 (10^6 cfu/ml) and 100 μl of ΦV10 phage (titer approximately 10^9 Plaque Forming Unit (PFU)/ml) were mixed with 50 ml of LB media and incubated overnight at 37°C, followed by centrifugation and filtration [27]. Phage lysate (titer approximately 10^9 PFU/ml) was then ultra-centrifuged at 35000 rpm in a rotor (Beckman SW41-Ti) for 2 hours using a 13 ml Beckman ultracentrifuge tube. The pellet was re-suspended in 0.85% saline and ultra-centrifuged again. The final pellet was re-suspended in 200 μl of 0.85% saline and stored at 4°C until use.

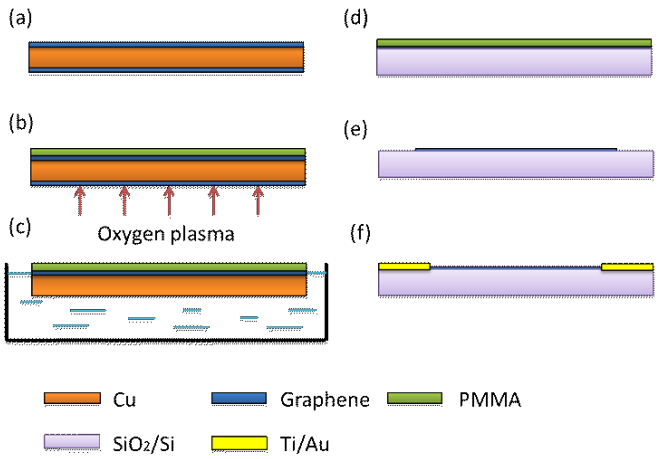

Fig. 5. Process flow of the device fabrication: (a) CVD growth of graphene on the copper foil; (b) removal of the backside graphene using the oxygen plasma etching, following the spin coating of the PMMA on the top side; (c) removal of the copper by wet etching; (d) transfer PMMA/graphene to the silicon substrate with thermal oxide grown on it; (e) removal of PMMA; (f) lithographically patterning the graphene channel and the deposition of contact electrodes using the e-beam evaporation.

C. Purification of TSP from phage ΦV10

25 ml phage was used for phage DNA isolation using a combination of the Qiagen Lambda phage isolation procedure and the Qiagen Genomic DNA Isolation Kit. Buffers L1 to L5 were made according to manufacturer's direction, followed by passage over the Qiagen genomic DNA isolation column (Qiagen). The sequences for the TSP of ΦV10 were amplified by PCR using primers designed from the published sequence of ΦV10 (NCBI, NC_007804). The amplified DNA was cloned into the pET-SUMO TA cloning vector (Invitrogen), facilitating an N-terminal fusion to an epitope tag containing 6 histidine residues (6S HIS-tag), which was subsequently used to facilitate purification of the protein. The plasmid construct was then transformed into Invitrogen DE3 chemically competent E. coli cells, followed by induction of E. coli to express the protein fragment by an addition of 1mM (isopropyl beta-D-thiogalactoside) (IPTG). Protein purification was performed using a Nickel agarose column (Ni-NTA purification system, Invitrogen). The clarified lysate was passed over a Ni-NTA column packed with 1.5 ml of nickel agarose slurry, washed and eluted. Fractions were verified by Simply Blue Safe Stain (Invitrogen) on an 8% polyacrylamide gel.

ACKNOWLEDGMENT

This material is based upon work supported by the National Science Foundation under Grant No. 1914420 (ECCS-CCSS program)

REFERENCES

[1] A. Garrido *et al.*, "A new multiplex real-time PCR developed method for Salmonella spp. and Listeria monocytogenes detection in food and environmental samples," *Food Control*, vol. 30, no. 1, pp. 76–85, Mar. 2013, doi: 10.1016/j.foodcont.2012.06.029.

[2] D. Mendes Silva and L. Domingues, "On the track for an efficient detection of Escherichia coli in water: A review on PCR-based methods," *Ecotoxicology and Environmental Safety*, vol. 113, pp. 400–411, Mar. 2015, doi: 10.1016/j.ecoenv.2014.12.015.

[3] C. Reiner-Rozman, M. Larisika, C. Nowak, and W. Knoll, "Graphene-based liquid-gated field effect transistor for biosensing: Theory and experiments," *Biosensors and Bioelectronics*, vol. 70, pp. 21–27, Aug. 2015, doi: 10.1016/j.bios.2015.03.013.

[4] S. J. Park, O. S. Kwon, S. H. Lee, H. S. Song, T. H. Park, and J. Jang, "Ultrasensitive Flexible Graphene Based Field-Effect Transistor (FET)-Type Bioelectronic Nose," *Nano Lett.*, vol. 12, no. 10, pp. 5082–5090, Oct. 2012, doi: 10.1021/nl301714x.

[5] Y. Liu, X. Dong, and P. Chen, "Biological and chemical sensors based on graphene materials," *Chem. Soc. Rev.*, vol. 41, no. 6, pp. 2283–2307, 2012, doi: 10.1039/C1CS15270J.

[6] A. Fokine and M. G. Rossmann, "Molecular architecture of tailed double-stranded DNA phages," *Bacteriophage*, vol. 4, no. 2, p. e28281, Apr. 2014, doi: 10.4161/bact.28281.

[7] X. Tan, H.-J. Chuang, M.-W. Lin, Z. Zhou, and M. M.-C. Cheng, "Edge Effects on the pH Response of Graphene Nanoribbon Field Effect Transistors," *J. Phys. Chem. C*, vol. 117, no. 51, pp. 27155–27160, Dec. 2013, doi: 10.1021/jp409116r.

[8] M. Pumera, "Graphene in biosensing," *Materials Today*, vol. 14, no. 7–8, pp. 308–315, Jul. 2011, doi: 10.1016/S1369-7021(11)70160-2.

[9] L. Zhu, M. Farhat, K. N. Salama, and P.-Y. Chen, "Two-dimensional materials-based radio frequency wireless communication and sensing systems for Internet-of-things applications," in *Emerging 2D Materials and Devices for the Internet of Things*, Elsevier, 2020, pp. 29–57. doi: 10.1016/B978-0-12-818386-1.00002-3.

[10] M. Hajizadegan *et al.*, "Graphene Sensing Modulator: Toward Low-Noise, Self-Powered Wireless Microsensors," *IEEE Sensors J.*, vol. 17, no. 22, pp. 7239–7247, Nov. 2017, doi: 10.1109/JSEN.2017.2737699.

[11] M. Kaisti, "Detection principles of biological and chemical FET sensors," *Biosensors and Bioelectronics*, vol. 98, pp. 437–448, Dec. 2017, doi: 10.1016/j.bios.2017.07.010.

[12] R. Hajian *et al.*, "Detection of unamplified target genes via CRISPR–Cas9 immobilized on a graphene field-effect transistor," *Nat Biomed Eng*, vol. 3, no. 6, pp. 427–437, Jun. 2019, doi: 10.1038/s41551-019-0371-x.

[13] G. Xu *et al.*, "Electrophoretic and field-effect graphene for all-electrical DNA array technology," *Nat Commun*, vol. 5, no. 1, p. 4866, Dec. 2014, doi: 10.1038/ncomms5866.

[14] P.-Y. Chen and A. Alù, "Atomically Thin Surface Cloak Using Graphene Monolayers," *ACS Nano*, vol. 5, no. 7, Art. no. 7, Jul. 2011, doi: 10.1021/nn201622e.

[15] P.-Y. Chen, C. Argyropoulos, and A. Alu, "Terahertz Antenna Phase Shifters Using Integrally-Gated Graphene Transmission-Lines," *IEEE Trans. Antennas Propagat.*, vol. 61, no. 4, pp. 1528–1537, Apr. 2013, doi: 10.1109/TAP.2012.2220327.

[16] P.-Y. Chen and A. Alu, "Terahertz Metamaterial Devices Based on Graphene Nanostructures," *IEEE Trans. THz Sci. Technol.*, vol. 3, no. 6, Art. no. 6, Nov. 2013, doi: 10.1109/TTHZ.2013.2285629.

[17] P.-Y. Chen and J. Jung, "P T Symmetry and Singularity-Enhanced Sensing Based on Photoexcited Graphene Metasurfaces," *Phys. Rev. Applied*, vol. 5, no. 6, Art. no. 6, Jun. 2016, doi: 10.1103/PhysRevApplied.5.064018.

[18] F. Chuang, P. Chen, T. Cheng, C.-H. Chien, and B. Li, "Improved field emission properties of thiolated multi-wall carbon nanotubes on a flexible carbon cloth substrate," *Nanotechnology*, vol. 18, no. 39, p. 395702, 2007.

[19] P.-Y. Chen, H. Huang, D. Akinwande, and A. Alu, "Graphene-based plasmonic platform for reconfigurable terahertz nanodevices," *Acs Photonics*, vol. 1, no. 8, pp. 647–654, 2014.

[20] M. E. Ramón *et al.*, "Three-Gigahertz Graphene Frequency Doubler on Quartz Operating Beyond the Transit Frequency," *IEEE Trans. Nanotechnology*, vol. 11, no. 5, pp. 877–883, Sep. 2012, doi: 10.1109/TNANO.2012.2203826.

[21] Han Wang, D. Nezich, Jing Kong, and T. Palacios, "Graphene Frequency Multipliers," *IEEE Electron Device Lett.*, vol. 30, no. 5, pp. 547–549, May 2009, doi: 10.1109/LED.2009.2016443.

[22] H. Huang *et al.*, "Chemical-sensitive graphene modulator with a memory effect for internet-of-things applications," *Microsyst Nanoeng*, vol. 2, no. 1, p. 16018, Dec. 2016, doi: 10.1038/micronano.2016.18.

[23] H. (Harry) Huang, M. Sakhdari, M. Hajizadegan, A. Shahini, D. Akinwande, and P.-Y. Chen, "Toward transparent and self-activated graphene harmonic transponder sensors," *Appl. Phys. Lett.*, vol. 108, no. 17, p. 173503, Apr. 2016, doi: 10.1063/1.4948254.

[24] N. Mohanty and V. Berry, "Graphene-Based Single-Bacterium Resolution Biodevice and DNA Transistor: Interfacing Graphene Derivatives with Nanoscale and Microscale Biocomponents," *Nano Lett.*, vol. 8, no. 12, pp. 4469–4476, Dec. 2008, doi: 10.1021/nl802412n.

[25] M. S. Mannoor *et al.*, "Graphene-based wireless bacteria detection on tooth enamel," *Nat Commun*, vol. 3, no. 1, p. 763, Jan. 2012, doi: 10.1038/ncomms1767.

[26] Y. Huang, X. Dong, Y. Liu, L.-J. Li, and P. Chen, "Graphene-based biosensors for detection of bacteria and their metabolic activities," *J. Mater. Chem.*, vol. 21, no. 33, p. 12358, 2011, doi: 10.1039/c1jm11436k.

[27] H. Handa, S. Gurczynski, M. P. Jackson, G. Auner, J. Walker, and G. Mao, "Recognition of Salmonella typhimurium by immobilized phage P22 monolayers," *Surface Science*, vol. 602, no. 7, pp. 1392–1400, Apr. 2008, doi: 10.1016/j.susc.2008.01.036.

[28] A. Singh *et al.*, "Bacteriophage tailspike proteins as molecular probes for sensitive and selective bacterial detection," *Biosensors and Bioelectronics*, vol. 26, no. 1, pp. 131–138, Sep. 2010, doi: 10.1016/j.bios.2010.05.024.

[29] P. Nguyen and V. Berry, "Graphene Interfaced with Biological Cells: Opportunities and Challenges," *J. Phys. Chem. Lett.*, vol. 3, no. 8, pp. 1024–1029, Apr. 2012, doi: 10.1021/jz300033g.

[30] W. Fu, L. Jiang, E. P. van Geest, L. M. C. Lima, and G. F. Schneider, "Sensing at the Surface of Graphene Field-Effect Transistors," *Adv. Mater.*, vol. 29, no. 6, p. 1603610, Feb. 2017, doi: 10.1002/adma.201603610.

[31] W. W. Wilson, M. M. Wade, S. C. Holman, and F. R. Champlin, "Status of methods for assessing bacterial cell surface charge properties based on zeta potential measurements," *Journal of Microbiological Methods*, vol. 43, no. 3, pp. 153–164, Jan. 2001, doi: 10.1016/S0167-7012(00)00224-4.

[32] R. J. Hunter, *Zeta potential in colloid science: principles and applications*. 1988. Accessed: Nov. 07, 2021. [Online]. Available: https://search.ebscohost.com/login.aspx?direct=true&scope=site&db=nlebk&db=nlabk&AN=877203

[33] M. Takahashi, "ζ Potential of Microbubbles in Aqueous Solutions: Electrical Properties of the Gas−Water Interface," *J. Phys. Chem. B*, vol. 109, no. 46, pp. 21858–21864, Nov. 2005, doi: 10.1021/jp0445270.

[34] Q. Luo, H. Wang, X. Zhang, and Y. Qian, "Effect of Direct Electric Current on the Cell Surface Properties of Phenol-Degrading Bacteria," *Appl Environ Microbiol*, vol. 71, no. 1, pp. 423–427, Jan. 2005, doi: 10.1128/AEM.71.1.423-427.2005.

[35] K. A. Soni, A. K. Balasubramanian, A. Beskok, and S. D. Pillai, "Zeta Potential of Selected Bacteria in Drinking Water When Dead, Starved, or Exposed to Minimal and Rich Culture Media," *Curr Microbiol*, vol. 56, no. 1, pp. 93–97, Jan. 2008, doi: 10.1007/s00284-007-9046-z.

[36] B. Li and B. E. Logan, "The impact of ultraviolet light on bacterial adhesion to glass and metal oxide-coated surface," *Colloids and Surfaces B: Biointerfaces*, vol. 41, no. 2–3, pp. 153–161, Mar. 2005, doi: 10.1016/j.colsurfb.2004.12.001.

[37] P. K. Ang, W. Chen, A. T. S. Wee, and K. P. Loh, "Solution-Gated Epitaxial Graphene as pH Sensor," *J. Am. Chem. Soc.*, vol. 130, no. 44, pp. 14392–14393, Nov. 2008, doi: 10.1021/ja805090z.

[38] T. Fang, A. Konar, H. Xing, and D. Jena, "Carrier statistics and quantum capacitance of graphene sheets and ribbons," *Appl. Phys. Lett.*, vol. 91, no. 9, p. 092109, Aug. 2007, doi: 10.1063/1.2776887.

[39] J. Guo, Y. Yoon, and Y. Ouyang, "Gate Electrostatics and Quantum Capacitance of Graphene Nanoribbons," *Nano Lett.*, vol. 7, no. 7, pp. 1935–1940, Jul. 2007, doi: 10.1021/nl0706190.

[40] X. Li *et al.*, "Large-Area Synthesis of High-Quality and Uniform Graphene Films on Copper Foils," *Science*, vol. 324, no. 5932, pp. 1312–1314, Jun. 2009, doi: 10.1126/science.1171245.

[41] X. Liang *et al.*, "Toward Clean and Crackless Transfer of Graphene," *ACS Nano*, vol. 5, no. 11, pp. 9144–9153, Nov. 2011, doi: 10.1021/nn203377t.

[42] L. L. Perry *et al.*, "Sequence analysis of *Escherichia coli* O157:H7 bacteriophage Î¦V10 and identification of a phage-encoded immunity protein that modifies the O157 antigen," *FEMS Microbiology Letters*, vol. 292, no. 2, pp. 182–186, Mar. 2009, doi: 10.1111/j.1574-6968.2009.01511.x.

[43] D. Scholl *et al.*, "An Engineered R-Type Pyocin Is a Highly Specific and Sensitive Bactericidal Agent for the Food-Borne Pathogen *Escherichia coli* O157:H7," *Antimicrob Agents Chemother*, vol. 53, no. 7, pp. 3074–3080, Jul. 2009, doi: 10.1128/AAC.01660-08.

Xuebin Tan received his B.S degree in Laser and Optical engineering from National University of Defense Technology, Hefei, China and M. Sc degree in Electrical and Electronics Engineering from Southeast University, Nanjing, China. He completed the Ph.D. degree in Wayne State University in 2014 for the Electrical and Electronics Engineering. He was then a postdoctoral scholar at Oregon State University. He currently serves as a product development engineer at Intel Corporation.

Minye Yang completed the bachelor's degree from Huazhong University of Science and Technology in Optical and Electronic Information, Hubei, China, in 2014, and received the M.Sc. degree in Electrical and Computer Engineering from Wayne State University, Detroit, MI, in 2019. He is currently pursuing the Ph.D. degree in Electrical and Computer Engineering at the University of Illinois at Chicago, Chicago, IL, USA.

His research focuses on applied electromagnetics, RF, microwave antennas and circuits, metasurfaces, wireless sensors and integrated systems.

Liang Zhu received his M.Sc. degree in optics from Sun Yat-Sen University, Guangzhou, China, in 2015. He completed the Ph.D. degree in University of Illinois at Chicago in 2021 for the Electrical and Electronics Engineering. His research mainly focuses on RF/microwave antennas and circuits, energy harvesting platforms and wireless sensors. He currently serves as an antenna engineer at Maxtena, Inc.

Gayathri Gunathilaka received the B.S. degree in Agriculture, Technology and Management from the University of Peradeniya, Sri Lanka, and the M. Sc. In Food Science and Nutrition from Wayne State University in 2014. She is currently a food safety regulatory specialist in Registrar Corp.

Zhixian Zhou received the B.S. degree in Physics from Lanzhou University, Lanzhou, China, and the Ph.D. degree from Florida State University, Tallahassee, FL, USA. He was a postdoctoral research associate with the Oak Ridge National Laboratory from 2005 to 2007. He joined Wayne State University (WSU) from 2007 to present and currently serves as a professor.

His research is centered on investigating the electrical transport properties and device physics of low dimensional materials, particularly two-dimensional van der Waals semiconductors including MoS2, MoSe2, WSe2, PdSe2 and black phosphorus.

Pai-Yen Chen (S'09, M' 13, SM' 17) is an Associate Professor in the Department of Electrical and Computer Engineering at the University of Illinois, Chicago (UIC). He received the Ph.D. degree from the University of Texas at Austin in 2013. He received M.S. and B.S. degrees from National Chiao Tung University in Taiwan in 2006 and 2004. He previously served as an Assistant Professor at the Wayne State University (WSU) during 2014-2018, a Research Scientist at Intellectual Ventures' Metamaterial Commercialization Center during 2013-2014, and a Research Staff in the National Nano Device Laboratory in Taiwan during 2006-2009. He has been involved in multidisciplinary research on applied electromagnetics, RF, microwave, millimeter-wave antennas and circuits, metamaterials, metasurfaces, wireless sensors and integrated systems, as well as nanoelectromagnetism in plasmonics and nanophotonics. He has received quite a few prestigious awards, including National Science Foundation (NSF) CAREER Award, IEEE Sensors Council Young Professional Award, IEEE Raj Mittra Travel Grant (RMTG) Award, SPIE Rising Researcher Award, ACES Early Career Award, PIERS Young Scientist Award, Young Scientist Awards from URSI General Assembly and URSI Commission B: Electromagnetics, IOP Measurement Science and Technology Emerging Leader, Air Force Research Laboratory Faculty Fellowship, UIC College of Engineering Faculty Research Award, WSU College of Engineering Faculty Research Excellence Award, Donald Harrington Fellowship, Taiwan Ministry of Education Study Abroad Award, United Microelectronics Corporation Scholarship, and quite a few best paper awards and travel grants from major IEEE conferences, including IEEE Antennas and Propagation Symposium (2011, 2013, 2016 and 2021), IEEE International Microwave Symposium (2015), IEEE Sensors Conference (2016), IEEE Wireless Power Transfer Conference (2021), and USNC-URSI Ernest K. Smith Student Paper Award (2012). He currently serves as Associate Editor of IEEE Sensors Journal, IEEE Transactions on Antennas and Propagation, IEEE Journal of Radio Frequency Identification (IEEE JRFID), IEEE Journal of Electromagnetics, RF and Microwaves in Medicine and Biology (IEEE-JERM), and Guest Editor of several international journals including IEEE Transactions on Antennas and Propagation. He was a former Associate Editor of Applied Electromagnetics. He was founder and chair of IEEE Sensors Council Chicago Chapter (2019-2021). He serves on the ACES Board of Directors (2021-2024).

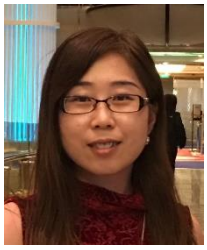

Yifan Zhang received the B.S. degree in medical from Shandong Medical University, Jinan, China, and the M. Med. Degree from the Chinese Center for Disease Control and Prevention, Beijing, China. She completed the Ph. D. degree in Food Science from the University of Maryland-College Park. She was then a Postdoctoral scholar in Ohio Agricultural Research and Development Center in the Ohio State University.

Her research focuses on microbial food safety including the prevalence and persistence of antimicrobial resistance in food and agriculture; phage as a reservoir and transmission vehicle of antimicrobial resistance; food safety and sustainability in urban agriculture; development of novel food safety control.

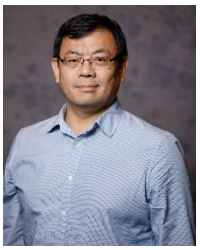

Mark Ming-Cheng Cheng received the B.S. and Ph.D. degrees from National Tsing-Hua University, Hsinchu, Taiwan, in 1995 and 2003, respectively. He was a Research Assistant Professor with the Department of Nanomedicine and Biomedical Engineering, the University of Texas Health Science Center at Houston, Houston, TX, USA, from 2006 to 2007. In 2008, he joined Wayne State University (WSU) and became a Full Professor in 2019. At WSU, he initialized curriculum in Nanoengineering and Cyber-Physical Systems (CPS). In 2019, he joined the Department of electrical and Computer Engineering, the university of Alabama, Tuscaloosa, AL, USA, where he is currently a professor. He has authored approximately 120 articles in peer-reviewed journal and conference proceedings. He has been involved in multidisciplinary research in microsystem design, biomedical devices, biosensor, new materials, wearable sensors, and environmental Interne-of-Things (IoT).

Dr. Cheng was a recipient of the National Science (NSF) CAREER Award, the ONR Summer Faculty Fellowship, and the President Research Enhancement Award.